

Numerical analysis of composite structures: creep, aging and failure

Severino P. C. Marques

Department of Civil Engineering, UFAL, AL – Brazil

Branca F. Oliveira

Laboratory of Virtual Design, UFRGS, RS – Brazil

Roberto C. Pavan and Guillermo J. Creus

CEMACOM-UFRGS, RS – Brazil

Abstract

The present work describes some results of a research program on the numerical modeling of structures in composite material, developed along the last years by a team at CEMACOM-UFRGS. Formulation for anisotropic viscoelastic behavior (including the effect of aging) and anisotropic damage are combined and implemented into a FE program that allows the analysis of shell structures in the context of finite displacements with small strains. Four numerical examples used for validation and verification are included.

1 Introduction

Composites with polymeric matrix and particularly those with fiber reinforcement, that provide higher (and taylorable) strength/weight ratio and additional advantages in terms of corrosion and fatigue tolerance, are increasingly present in naval, aeronautical, mechanical and civil structures. In the last years, analytical and computational models have been developed that allow to model the effective behavior of complex structures and to optimize composite properties.

A number of models have been already proposed for the prediction of the elastic modulus of composites, as reviewed by [1] and [2]. The Mori-Tanaka technique [3] can be used with relative accuracy even for periodic structures if the volume fraction is moderate [4]. Current research work is directed to model more complex behavior, as viscoelasticity (linear and nonlinear), aging and damage.

Viscoelasticity: The analysis by [5] shows that the viscoelastic effect in unidirectional fiber-composites is particularly significant for axial shear, transverse shear and transverse axial stress, matrix-dominated properties. The viscoelastic response becomes more pronounced under conditions of high temperature, sustained loading, and/or high stress level.

Aging: The term aging refers to the change of material properties with age and can be broadly classified as physical or chemical. During physical aging the mobility of the chain segments is hindered, and the material becomes stiffer, so that at a given time the compliance is decreased over that of a viscoelastic material without aging [6]. Chemical aging produces different (generally opposite) effects [7].

Some works model the effect of viscoelasticity using the elastic-viscoelastic correspondence principle [8], applied through Laplace transforms. Laplace transforms are not adequate to be used in age-dependent problems, where the kernel in the integral representation is not of the closed-cycle type. Sometimes, the effect of aging may be approximated using Laplace transforms associated with time shifting techniques. Still, this procedure is not adequate in some important cases [9]. Laplace transform techniques are also inadequate to model nonlinear effects (as those related to damage). Thus, in this work incremental real time analysis is used.

Damage: Swirlmat composites exhibit viscoelastic behavior as well as profuse microcracking and stiffness reduction under increasing loads. Its behavior may be modeled by means of isotropic continuum damage theory [10]. Composite laminates with unidirectional fibers (as pultruded sections [11]), show similar characteristics but highly anisotropic behavior. This type of behavior is addressed in Section 4 using an anisotropic damage theory

Numerical analysis: in the context of structural analysis of complex shape structures by numerical techniques (as the Finite Elements or Boundary Elements methods), the use of more general constitutive equations (to be integrated numerically) seems adequate. In Section 5 formulations implemented into a Finite Element program for the analysis of composite plates and shells, including effects of geometrical nonlinearity, viscoelasticity, aging and damage are reviewed.

This research is addressed to structural composites of polymeric matrix and thus a context of small strains with finite displacements is adequate.

2 Experimental background

Composite laminates are known to sustain multiple damage modes under monotonic loading, most of which by are not critical by themselves but may combine or lead to other mechanisms causing failure. Some experimental work has been done on damage and failure of composites at room and higher temperatures (see for example, [12] and [13]). In reference [10] useful results can be found. For example, Fig 1 shows the effect of the creep stress on the normalized instantaneous compliance and Fig. 2 shows the effect of the creep stress on the permanent creep stress after load removal.

The behavior corresponding to “softening” aging (e.g. stiffness loss) is similar to that associated damage. In this work, we follow the usual trend and reserve the word damage to changes associated with stress and strain increments.

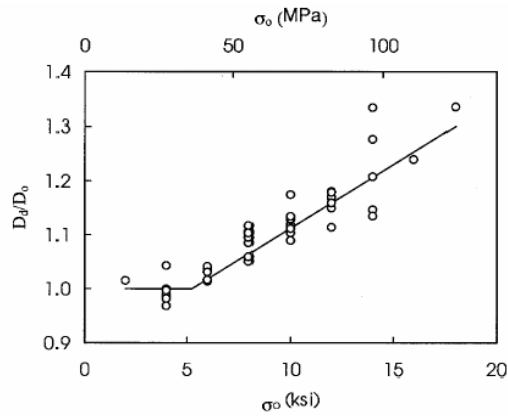


Figure 1: The effect of creep stress σ_0 on the normalized instantaneous compliance, as given by the ratio D_d/D_0 , where D_d is the damaged compliance evaluated during unloading.

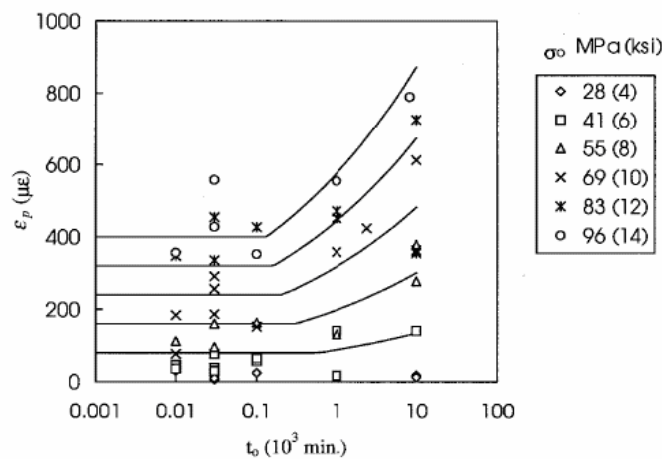


Figure 2: The effect of creep stress σ_0 and load duration t_0 the permanent strain ϵ_p reduced at times $3t_0$ after load removal (t_0 in 10^3 min, ϵ_p in $\mu\epsilon$).

3 Linear aging viscoelastic formulation

3.1 General relations

A general relation for a linearly viscoelastic aging material can be written in the history-dependent (uniaxial) form [14]

$$\varepsilon(t) = \int_{\tau_0}^t D(t, \tau) \dot{\sigma}(\tau) d\tau = \frac{\sigma(t)}{E(t)} - \int_{\tau_0}^t \frac{\partial D(t, \tau)}{\partial \tau} \sigma(\tau) d\tau \quad (1)$$

$D(t, \tau)$ is the response to a unit stress $\sigma(t) = H(t - \tau)$ applied at time τ . The representation above is the basic general integral representation that uses the concept of compliance. Others representations exist, among them those based on dynamic modulus [8]. In theory these representations are equivalent, but in practice (due experimental limitations and inaccuracies) they are not. For structural materials under static load and expected long service lives, the use of a compliance based representation is more convenient. $D(t, \tau)$ has instantaneous and deferred components, whose separation is a matter of convention to be discussed in each case. For non-aging viscoelastic materials it is

$$D(t, \tau) = D(t - \tau) = \frac{1}{E} + C(t - \tau) \quad (2)$$

For ageing materials two situations may arise. The first one corresponds to materials that become stiffer with age. In this case it is written

$$D(t, \tau) = \frac{1}{E(\tau)} + C(t, \tau) \quad (3)$$

with $\partial E(\tau)/\partial \tau > 0; \partial C(t, \tau)/\partial \tau < 0$. The instantaneous part in the creep compliance is a function of the delayed time τ as the new bonds are initially unstressed and only react to incremental loads. In absence of creep $C(t, \tau) = 0$. Substitution of (3) into (1) yields

$$\varepsilon(t) = \int_{\tau_0}^t \frac{1}{E(\tau)} \dot{\sigma}(\tau) d\tau = \frac{\sigma(t)}{E(t)} - \int_{\tau_0}^t \frac{1}{E(\tau)} \sigma(\tau) d\tau \quad (4)$$

or, in rate form,

$$\dot{\varepsilon}(t) = \frac{\dot{\sigma}(t)}{E(t)} \quad (5)$$

For materials whose stiffness degrades with age, the instantaneous part is a function of the current time t

$$D(t, \tau) = \frac{1}{E(t)} + C(t, \tau) \quad (6)$$

with $\partial E(t)/\partial t < 0; \partial C(t, \tau)/\partial t > 0$. For $C(t, \tau) = 0$,

$$\varepsilon(t) = \frac{\sigma(t)}{E(t)} \quad (7)$$

or, in rate form

$$\dot{\varepsilon}(t) = \frac{\dot{\sigma}(t)}{E(t)} - \frac{\sigma(t) \dot{E}(t)}{E^2(t)} \quad (8)$$

Both types of behavior, as represented by equations (5) and (8) are illustrated in Fig. 3. It should be noticed that aging involves, even in the absence of creep, history dependence and residual strains,

features not usually associated with elastic behavior. Ageing introduces a kind of nonlinearity apparent in loading-unloading processes. In particular, (5) has the form of a hypoelastic relationship [15].

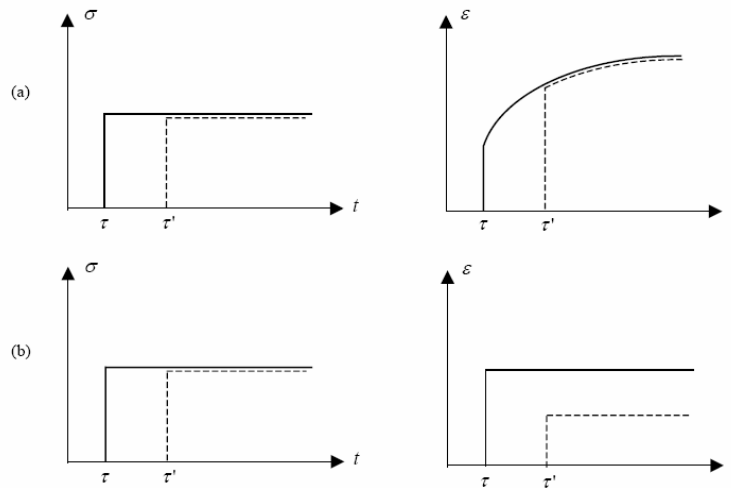


Figure 3: Instantaneous behavior of softening and hardening materials. Typical response in strain for a one-step loading. (a) case $\dot{E} < 0$. (b) case $\dot{E} > 0$

3.2 Representation by means of state variables

Softening case: the creep compliance function in (1) is approximated through a Dirichlet-Prony exponential series as

$$\dot{D}(t, \tau) = \sum_{i=1}^n \frac{1}{\eta_i(\tau)} e^{-(t-\tau)/\theta_i} \tag{9}$$

Defining a state variable as

$$q_i(t) = \int_{\tau_0}^t \frac{\dot{\sigma}(\tau)}{\eta_i(\tau)} e^{-(t-\tau)/\theta_i} d\tau \tag{10}$$

Eq. (1) may be written

$$\dot{\epsilon}(t) = \frac{\dot{\sigma}(t)}{E(t)} + \sum_{i=1}^n q_i(t) \tag{11}$$

In terms of rheology models, equation (11) corresponds to a spring with a time-dependent elastic modulus and “ n ” Kelvin elements with time-dependent parameters in series.

Hardening case: In the hardening case we must work incrementally. From (1)

$$\dot{\varepsilon}(t) = \int_{\tau_0}^t \frac{\dot{\sigma}(\tau)}{\eta(\tau)} e^{-(t-\tau)/\theta} d\tau \quad (12)$$

Approximating the derivative of the creep compliance function through a Dirichlet-Prony exponential series as

$$\dot{D}(t, \tau) = \sum_{i=1}^n \frac{1}{\eta_i(\tau)} e^{-(t-\tau)/\theta_i} \quad (13)$$

and defining the state variable in the following form

$$q_i(t) = \int_{\tau_0}^t \frac{\dot{\sigma}(\tau)}{\eta_i(\tau)} e^{-(t-\tau)/\theta_i} d\tau \quad (14)$$

it is then possible to write

$$\dot{\varepsilon}(t) = \frac{\dot{\sigma}(t)}{E(t)} + \sum_{i=1}^n q_i(t) \quad (15)$$

3.3 Extension to multiaxial situations

The uniaxial relation (1) has to be generalized to

$$\varepsilon_i(t) = \int_0^t D_{ij}(t, \tau) \frac{\partial \sigma_j(\tau)}{\partial \tau} d\tau, \quad i, j = 1, 2, \dots, 5 \quad (16)$$

In this work the composite material is modeled as linear viscoelastic, with orthotropic symmetry [16]. Then $\varepsilon_i(t)$ are the components of the strain vector $\{\varepsilon\} = \{\varepsilon_{11}, \varepsilon_{22}, 2\varepsilon_{12}, 2\varepsilon_{13}, 2\varepsilon_{23}\}$ and $\sigma_j(t)$ are the components of the stress vector $\{\sigma\} = \{\sigma_{11}, \sigma_{22}, \sigma_{12}, \sigma_{13}, \sigma_{23}\}$, at time t . Components ε_{33} and σ_{33} are not considered. $D_{ij}(t, \tau)$ are the creep functions corresponding to components ε_i and σ_j . Upon integration by parts, equation (16) may be written

$$\varepsilon_i(t) = D_{ij}(t, t)\sigma_j(t) - \int_0^t \frac{\partial}{\partial \tau} D_{ij}(t, \tau)\sigma_j(\tau) d\tau \quad (17)$$

Approximating the creep functions by a Dirichlet-Prony series it can be written

$$D_{ij}(t, \tau) = D_{ij}^0 + \sum_{p=1}^M D_{ij}^p \left[1 - \exp\left(-\frac{t-\tau}{\theta_{ij}^p}\right) \right] \quad (18)$$

where D_{ij}^0 , D_{ij}^p and θ_{ij}^p are parameters to be determined from experimental results. M is the number of significant terms in the series and depends on the accuracy desired. The parameters θ_{ij}^p are the retardation times.

4 Damage formulation

4.1 Anisotropic damage and effective stresses

According to Murakami [17] proposal, a relation between the global stress tensor σ_{ij} and the effective stress tensor $\bar{\sigma}_{ij}$ is given by the linear transformation

$$\bar{\sigma}_{ij} = M_{ijkl}\sigma_{kl} \quad (19)$$

where M_{ijkl} is a fourth order damage effective tensor. For a generic state of strain and damage, the stress effective tensor $\bar{\sigma}_{ij}$ is usually no symmetrical. A symmetrical form for $\bar{\sigma}_{ij}$ it is obtained through the equation

$$\bar{\sigma}_{ij} = \frac{1}{2} \left[\sigma_{ik} (\delta_{kj} - \phi_{kj})^{-1} + (\delta_{il} - \phi_{il})^{-1} \sigma_{lj} \right] \quad (20)$$

where δ_{ij} is the delta de Kronecker and ϕ_{ij} is a second order damage tensor [18]. For the case of plane stress, $\sigma_{33} = \sigma_{13} = \sigma_{23} = \phi_{33} = \phi_{13} = \phi_{23} = 0$ and the representation of the damage effective tensor [M] is reduced to

$$[M] = \frac{1}{\Delta} \begin{bmatrix} \psi_{22} & 0 & \phi_{12} \\ 0 & \psi_{11} & \phi_{12} \\ \frac{1}{2}\phi_{12} & \frac{1}{2}\phi_{12} & \frac{\psi_{11}+\psi_{22}}{2} \end{bmatrix} \quad (21)$$

with $\Delta = \psi_{11}\psi_{22} - \phi_{12}^2$ and $\psi_{ij} = \delta_{ij} - \phi_{ij}$.

4.2 Constitutive equations for elastic damage

The elastic relations, for the cases of undamaged and damaged material are

$$\bar{\sigma}_{ij} = E_{ijkl}\bar{\varepsilon}_{kl} \quad (22)$$

$$\sigma_{ij} = \bar{E}_{ijkl}\varepsilon_{kl} \quad (23)$$

Using the hypothesis of equivalent elastic energy [19] it is shown that

$$\bar{E}_{ijkl} = M_{pqkl}^{-1} E_{rspq} M_{rsij}^{-1} \quad (24)$$

and (bar indicate effective values)

$$\bar{\varepsilon}_{ij} = M_{ijpq}^{-1} \varepsilon_{pq} \quad (25)$$

4.3 Constitutive relations for incremental analysis

For incremental analyses in non-linear situations, constitutive relations in incremental form are needed. Differentiating equation (23) in relation to time,

$$\dot{\sigma}_{ij} = \left(M_{pqkl}^{-1} E_{rspq} M_{rsij}^{-1} \right) \dot{\varepsilon}_{kl} + \overline{\left(M_{pqkl}^{-1} E_{rspq} M_{rsij}^{-1} \right)} \varepsilon_{kl} \quad (26)$$

$$\dot{\sigma}_{ij} = \left(M_{pqkl}^{-1} E_{rspq} M_{rsij}^{-1} \right) \dot{\varepsilon}_{kl} + \left(\left(\dot{M}_{pqkl}^{-1} E_{rspq} M_{rsij}^{-1} \right) + \left(M_{pqkl}^{-1} \dot{E}_{rspq} M_{rsij}^{-1} \right) + \left(M_{pqkl}^{-1} E_{rspq} \dot{M}_{rsij}^{-1} \right) \right) \varepsilon_{kl} \quad (27)$$

And, as $M_{pqkl}^{-1} \dot{E}_{rspq} M_{rsij}^{-1} = 0$,

$$\dot{\sigma}_{ij} = \left(M_{pqkl}^{-1} E_{rspq} M_{rsij}^{-1} \right) \dot{\varepsilon}_{kl} + \left(\dot{M}_{pqkl}^{-1} E_{rspq} M_{rsij}^{-1} + M_{pqkl}^{-1} E_{rspq} \dot{M}_{rsij}^{-1} \right) \varepsilon_{kl} \quad (28)$$

From the symmetry of the damage tensor we obtain,

$$\dot{\sigma}_{ij} = \left(M_{pqkl}^{-1} E_{rspq} M_{rsij}^{-1} \right) \dot{\varepsilon}_{kl} + 2 \left(\dot{M}_{pqkl}^{-1} E_{rspq} M_{rsij}^{-1} \right) \varepsilon_{kl} \quad (29)$$

Using the chain rule,

$$\dot{M}_{pqkl}^{-1} = \frac{\partial M_{pqkl}^{-1}}{\partial \phi_{pq}} \frac{\partial \phi_{pq}}{\partial \varepsilon_{kl}} \dot{\varepsilon}_{kl} \quad (30)$$

Therefore,

$$\dot{\sigma}_{ij} = \left(M_{pqkl}^{-1} E_{rspq} M_{rsij}^{-1} \right) \dot{\varepsilon}_{kl} + 2 \left(\left(\frac{\partial M_{pqkl}^{-1}}{\partial \phi_{pq}} \frac{\partial \phi_{pq}}{\partial \varepsilon_{kl}} \dot{\varepsilon}_{kl} \right) E_{rspq} M_{rsij}^{-1} \right) \varepsilon_{kl} \quad (31)$$

$$\dot{\sigma}_{ij} = \left[\left(M_{pqkl}^{-1} E_{rspq} M_{rsij}^{-1} \right) + \left(2 \left(\frac{\partial M_{pqkl}^{-1}}{\partial \phi_{pq}} \frac{\partial \phi_{pq}}{\partial \varepsilon_{kl}} \right) E_{rspq} M_{rsij}^{-1} \varepsilon_{kl} \right) \right] \dot{\varepsilon}_{kl} \quad (32)$$

To obtain an explicit relation form, it is necessary to introduce a relation for the damage ϕ . Let us consider the uniaxial case. The exponential equation $\bar{E} = E e^{-K\varepsilon}$ is used to model the degradation of the elastic modulus, K being a constant to be determined experimentally. Then, the damage coefficients are obtained by the expression (24):

$$\phi = 1 - \sqrt{\frac{\bar{E}}{E}} = 1 - \sqrt{\frac{E e^{-K\varepsilon}}{E}} = 1 - \sqrt{e^{-K\varepsilon}} \quad (33)$$

For the uniaxial case, (26) reduces to

$$\dot{\sigma} = \bar{E} \dot{\varepsilon} + \dot{\bar{E}} \varepsilon \quad (34)$$

then,

$$\dot{\bar{E}} = \frac{\partial \bar{E}}{\partial \varepsilon} \dot{\varepsilon} = -K E e^{-K\varepsilon} \dot{\varepsilon} \quad (35)$$

and substituting in (34),

$$\dot{\sigma} = E e^{-K\varepsilon} (1 - K\varepsilon) \dot{\varepsilon} \quad (36)$$

4.4 Stress concentration tensors

In the following, the equations of Mori-Tanaka [3] are used to find the stress in the fibers. In agreement with this theory, the stresses in the fibers are equivalent to the stress obtained through an equivalent inclusion.

The expressions for the stress and strain concentration tensor B^F and A^F , respectively, for the fibers are

$$A_{ijkl}^F = \left[I_{ijkl} + c^M S_{ijrs} E_{rsmn}^{M-1} (E_{mnkl}^F - E_{mnkl}^M) \right]^{-1} \quad (37)$$

$$B_{ijkl}^F = \left[I_{ijkl} + c^M E_{ijmn}^M (I_{mnpq} - S_{mnpq}) (E_{pqkl}^{F-1} - E_{pqkl}^{M-1}) \right]^{-1} \quad (38)$$

where $[S]$ it is the Eshelby tensor (fourth order) for the elastic case, $[I]$ it is the identity tensor (fourth order), c^M and c^F are the fractions of the volume corresponding, respectively, the matrix and the fiber.

Substituting (37) and (38) in the equations (39) and (40) we obtain the stress and strain concentration tensor B^M and A^M , respectively, for the matrix:

$$c^M A_{ijkl}^M + c^F A_{ijkl}^F = I_{ijkl} \quad (39)$$

$$c^M B_{ijkl}^M + c^F B_{ijkl}^F = I_{ijkl} \quad (40)$$

Mura [20] provides the non-null components of tensor $[S]$ for fibers with circular cross-section.

5 Finite element formulation and solution

We follow the general procedure [16, 21], including the effects of viscoelastic and hygrothermal deformations. As seen in [16] this leads to an incremental relation of the form

$$([\mathop{K}_T^k]) \{U\} = \{^{k+1}P\} - \{^kF\} + \{ {}_0F^v \} + \{ {}_0F^T \} + \{ {}_0F^H \} \quad (41)$$

where $[\mathop{K}_T^k]$ is the tangent stiffness matrix corresponding to step k , $\{^{k+1}P\}$ is the vector of external nodal forces at step $k+1$, $\{^kF\}$ is the vector of nodal point forces equivalent to the element stresses at the step k and, finally, $\{ {}_0F^v \}$, $\{ {}_0F^T \}$ and $\{ {}_0F^H \}$ are the vectors of viscoelastic, thermal and hygroscopic loads, respectively.

The numerical solution of the problem is implemented through an incremental-iterative procedure. For the solution of the non-linear equilibrium equations, we use the Newton-Raphson Method or the Generalized Displacement Control Method proposed by [22].

6 Verification and validation

Some few examples are shown here for the viscoelastic aging and damage formulations. Other examples of the application of the FE program have been published elsewhere [15, 16, 23–25].

6.1 Creep buckling of beam columns considering aging effects

A beam column example has been analyzed to show the effect of aging, both of the “hardening” and “softening” types. The beam column has a length of 320 mm, a section 40 mm wide and 20 mm thick and initial curvature with 20mm central sag. The material is viscoelastic with the constitutive relations given by (5) and (8) respectively.

The results, in the form of plots deflection-time are shown in Fig. 4 and indicate the effect of aging; coincidence between numerical and analytical solutions is apparent. More details and other numerical and analytical solutions may be found in [15].

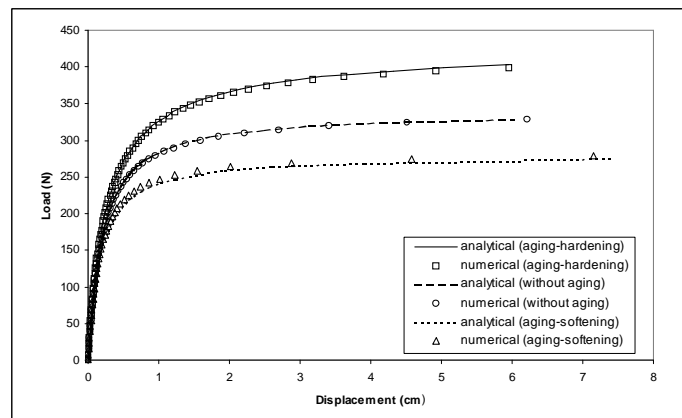


Figure 4: Creep-buckling deflections of beam columns in aging material

6.2 Verification of the integration procedure for incremental damage

To verify the incremental equation and the integration procedure implemented into the FE program, an isotropic plate subject to axial traction is analyzed. Numerical and analytical results are shown in Fig. 5.

6.3 Validation of the numerical damage analysis for a unidirectional composite

The present formulation can be used to determine stresses in each constituent (fiber and matrix) of the composite. In this example, we consider a plate under uniaxial tension. Experimental details and mechanical properties of the materials are ($E^F = 410000.00MPa$ e $E^M = 80000.00MPa$) [13]. Other properties were determined using mixture theory [11]. As the plate is under axial tension only one K_{ij} parameter for each matrix and fiber are needed: $K_{11} = K_{11}^F = K_{11}^M = 50$. In figure 5 the comparison between numerical and experimental results may be seen.

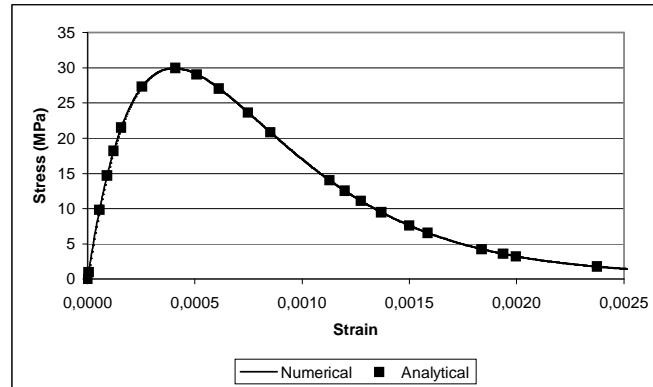


Figure 5: Relation stress x strain and incremental numeric approach ($E=200\text{GPa}$, $K=2500$)

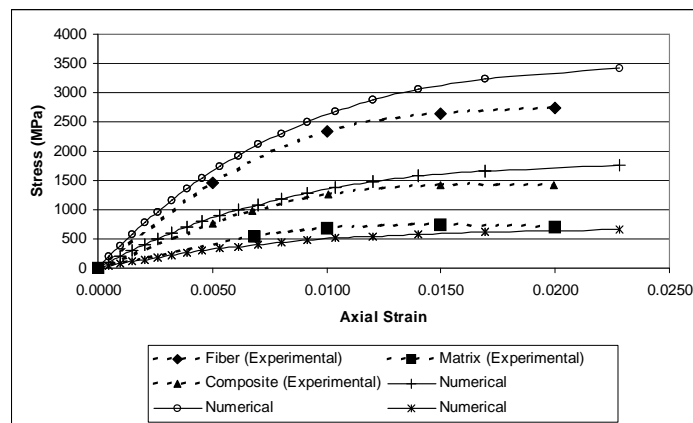


Figure 6: Comparison of numerical and experimental results for composite and components.

6.4 Viscoelasticity and damage

This example corresponds to the representation of damage combined with viscoelastic behavior. A square plate of side 10 cm and thickness 0.2 cm, was modelled with one nine-node element with 2×2 integration points. The material properties are: $E_{11} = 2.0\text{GPa}$ $\nu_{12} = 0.30$ $\theta = 100$ min. The figure 6 represents the increase of strain in time for $K=250$ and different values of uniaxial stress. The behavior shown represents (qualitatively) the behavior observed in tests.

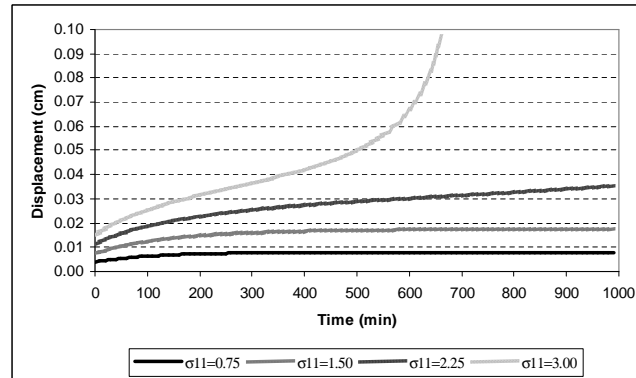


Figure 7: Displacement x time for different tension ($K=250$)

7 Conclusions and final remarks

Formulation and numerical examples are shown for composite materials, focusing viscoelastic, age and damage effects. The corresponding constitutive equations are implemented into a nonlinear FE code for plate and shell structures.

Although the examples given are limited to simple situations (for the purpose of verification of the numerical models), the FE program may be used with more complex structures, as shown in [15, 16, 23, 24], where additional information on the numerical code is also provided.

In relation to the viscoelastic damage formulation, the extension of the current work to other load histories would require empirical information on each term of the damage tensor. Otherwise, we may try to define a “damage surface” akin to the yield surface in plasticity theory. For the viscoelastic case, this surface has to be defined in the strain space. Work on this subject is under way and will be published elsewhere.

Acknowledgements

The financial support of CAPES, PROPESQ, CNPq and UNOCHAPECÓ is gratefully acknowledged. Remarks by the referee have been taken into account and are sincerely appreciated.

References

- [1] Hashin, Z., On elastic behaviour of fibre reinforced materials of arbitrary transverse. *J Mech Phys Solids*, **13**, pp. 119–134, 1965. Phase geometry.
- [2] Christensen, R.M., *Mechanics of Composite Materials*. Wiley, 1979.
- [3] Mori, T. & Tanaka, K., Average stress in matrix and average elastic energy of materials with misfitting

- inclusions. *Acta Metallurgica*, **21**, pp. 571–574, 1973.
- [4] Brinson, L.C. & Lin, W.S., Comparison of micromechanics methods for effective properties of multiphase viscoelastic composites. *Composite Structures*, **41**, pp. 353–367, 1998.
- [5] Hashin, Z., Viscoelastic fiber reinforced materials. *AIAA Journal*, **4(1411-1417)**, 1966.
- [6] Brinson, L.C. & Gates, T.S., Effects of physical aging on long term creep of polymers and polymer matrix composites. *Int J Solids Structures*, **32**, pp. 827–846, 1995.
- [7] Liao, K., Schultheisz, C.R., Hunston, D.L. & Brinson, L.C., Long-term durability of fiber-reinforced polymer-matrix composite materials for infrastructure applications: A review. *Journal of Advanced Materials*, **30(4)**, pp. 3–40, 1998.
- [8] Lakes, R.S., *Viscoelastic Solids*. CRC, 1999.
- [9] Brinson, L.C. & Fisher, F.T., Viscoelastic interphases in polymer-matrix composites: theoretical models and finite-element analysis. *Composites Science and Technology*, **61(731-748)**, 2001.
- [10] Smith, L.V. & Weitsman, Y.J., The visco-damage mechanical response of swirl-mat composites. *International Journal of Fracture*, **97**, pp. 301–319, 1999.
- [11] Barbero, E.J., *Introduction to Composite Materials Design*. Taylor and Francis: Philadelphia - PA, 1998.
- [12] Daniel, I.M. & Lee, J.W., Damage development in composite laminates under monotonic loading. *Journal of Composites Technology and Research*, **12(2)**, pp. 98–102.
- [13] Akshantala, N.V. & Brinson, L.C., Experimental study of viscoelastic effects and aging on elevated temperatures damage and failure of polymer composites. *Mechanics of Time-Dependent Materials*, pp. 1–19, 2003.
- [14] Creus, G.J., *Viscoelasticity - Basic Theory and Applications to Concrete Structures*. Springer-Verlag: Heidelberg, 1986.
- [15] Oliveira, B.F. & Creus, G.J., An analytical-numerical framework for the study of ageing in fibre reinforced polymer composites. *Composite Structures*, **65**, pp. 443–457, 2004.
- [16] Marques, S.P.C. & Creus, G.J., Geometrically nonlinear finite elements analysis of viscoelastic composite materials under mechanical and hicrothermal loads. *Computers & Structures*, **53**, pp. 449–456, 1994.
- [17] Murakami, S., Notion of continuum damage mechanics and its application to anisotropic creep damage theory. *Journal of Engineering Mechanics and Technology*, **105**, pp. 99–105, 1983.
- [18] Voyiadjis, G.Z. & Kattan, P.I., *Advances in Damage Mechanics: Metals and Metal Matrix*. Elsevier: Amsterdam, 1999. Composites.
- [19] Sidoroff, F., Description of anisotropic damage application to elasticity. *IUTAM Colloquium on Physical Nonlinearities in Structural Analysis*, pp. 237–244, 1981.
- [20] Mura, T., *Micromechanics of defects in Solids*. Martinus Nijhoff Publishers, 1982.
- [21] Bathe, K.J., *Finite Element Procedures*. Prentice-Hall: Englewood Cliffs - New Jersey, 1996.
- [22] Yang, Y.B. & Shieh, M.S., Solution method for nonlinear problems with multiple critical points. *AIAA Journal*, **28(12)**, pp. 2110–2116, 1990. (see also S.R. Kuo and Y.B. Yang Tracing Postbuckling Paths of Structures Containing Multi-loops. *International Journal for Numerical Methods in Engineering* 1995; 38:4053-4075).
- [23] Oliveira, B.F. & Creus, G.J., Viscoelastic failure analysis of composite plates and shells. *Composite Structures*, **49(4)**, pp. 369–384, 2000.
- [24] Oliveira, B.F. & Creus, G.J., Nonlinear viscoelastic analysis of thin walled beams in composite material. *Thin-Walled Structures*, **41**, pp. 891–917, 2003.
- [25] Pavan, R.C. & Creus, G.J., Anisotropic damage in composite shell structures. *Latin American Journal of Solids and Structures*, **3**, pp. 263–278, 2006.

